Drug Design, Development and Therapy

Dovepress
open access to scientific and medical research

Open Access Full Text Article

ORIGINAL RESEARCH

Shen'ge Formula Protects Cardiac Function in Rats with Pressure Overload-Induced Heart Failure

Boyong Qiu[1,2,*], Siyu Qiao[2,*], Xiujuan Shi[2], Lin Shen[2], Bing Deng[2], Zilin Ma[2], Duan Zhou[2], Yihong Wei[2]

[1]Heart Center/National Regional (Traditional Chinese Medicine) Cardiovascular Diagnosis and Treatment Center, The First Affiliated Hospital of Henan University of CM, Zhengzhou, Henan, People's Republic of China; [2]Cardiovascular Department, Longhua Hospital affiliated to Shanghai University of Traditional Chinese Medicine, Shanghai, People's Republic of China

*These authors contributed equally to this work

Correspondence: Yihong Wei; Duan Zhou, Email weiyihong2022@shutcm.edu.cn; zhouduan@126.com

Background: In China, Shen'ge formula (SGF), a Traditional Chinese Medicine blend crafted from ginseng and gecko, holds a revered place in the treatment of cardiovascular diseases. However, despite its prevalent use, the precise cardioprotective mechanisms of SGF remain largely uncharted. This study aims to fill this gap by delving deeper into SGF's therapeutic potential and underlying action mechanism, thus giving its traditional use a solid scientific grounding.

Methods: In this study, rats were subjected to abdominal aortic constriction (AAC) to generate pressure overload. Following AAC, we administered SGF and bisoprolol intragastrically at specified doses for two distinct durations: 8 and 24 weeks. The cardiac function post-treatment was thoroughly analyzed using echocardiography and histological examinations, offering insights into SGF's influence on vital cardiovascular metrics, and signaling pathways central to cardiac health.

Results: SGF exhibited promising results, significantly enhanced cardiac functions over both 8 and 24-week periods, evidenced by improved ejection fraction and fractional shortening while moderating left ventricular parameters. Noteworthy was SGF's role in the significant mitigation of myocardial hypertrophy and in fostering the expression of vital proteins essential for heart health by the 24-week mark. This intervention markedly altered the dynamics of the Akt/HIF-1α/p53 pathway, inhibiting detrimental processes while promoting protective mechanisms.

Conclusion: Our research casts SGF in a promising light as a cardioprotective agent in heart failure conditions induced by pressure overload in rats. Central to this protective shield is the modulation of the Akt/HIF-1α/p53 pathway, pointing to a therapeutic trajectory that leverages HIF-1α promotion and p53 nuclear transport inhibition.

Keywords: Shen'ge formula, heart failure, hypertrophy, apoptosis, angiogenesis

Introduction

Heart failure (HF) is a worldwide disease with high morbidity, rehospitalization, and mortality. Between 2013 and 2016, there were approximately 6.2 million HF patients ≥20 years of age in the USA.[1] The ESC-HF pilot study showed that the annual all-cause mortality rates were 17 and 7%, in hospitalized and stable HF patients, respectively, with corresponding annual hospitalization rates of 44 and 32%, respectively.[2] In China, approximately 13.7 million patients aged ≥35 years have HF, accounting for an incidence of approximately 1.3%.[3] Consequently, there is an urgent need to identify cardioprotective medicines for HF.

Myocardial hypertrophy and angiogenesis play essential roles in maintaining cardiac homeostasis. Pathological hypertrophy occurring in HF is accompanied by angiogenic dysfunction, which in turn leads to further heart remodeling.[4,5] Studies have shown that effective inhibition of myocardial pathological hypertrophy and promotion of angiogenesis will help improve ventricular remodeling.[6,7] Apoptosis also plays a key role in the complex mechanisms of HF. The inhibition of apoptotic pathways can improve left ventricular remodeling in the progression of HF,[8] and the apoptotic protein p53 plays an essential

Received: 10 January 2024
Accepted: 20 May 2024
Published: 30 May 2024

Graphical Abstract

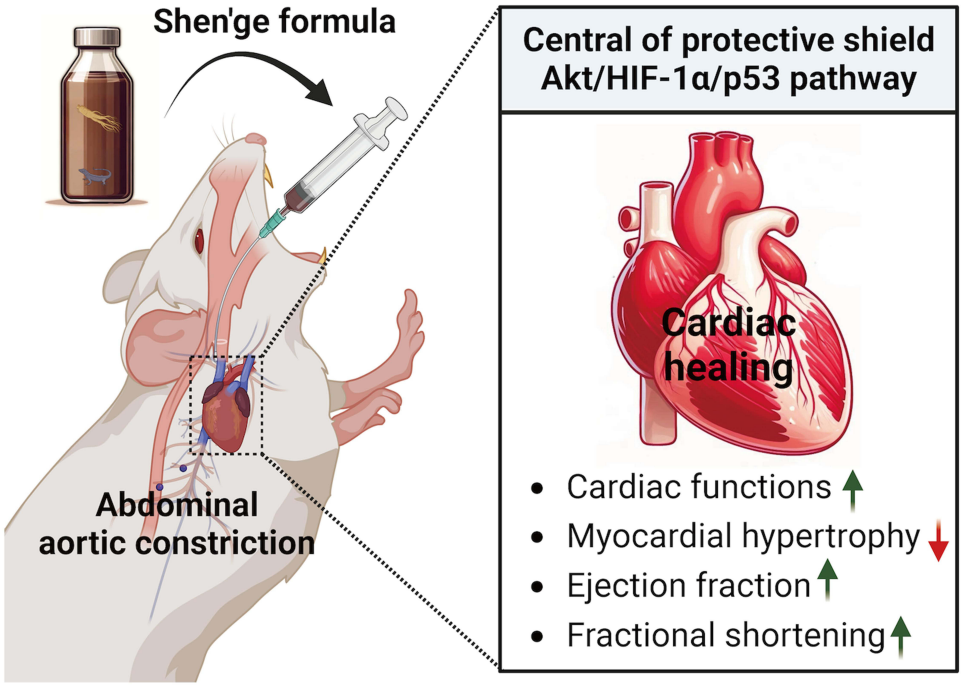

role in this process.[9] p53 cannot only regulate caspase 3, Bax, and Bcl-2 to regulate apoptosis,[10] but is also closely related to myocardial apoptosis, hypertrophy, and angiogenesis in the progression of HF.[11,12]

Shen'ge formula (SGF), a traditional Chinese medicine (TCM) formula consisting of ginseng and gecko in a 3:1 weight ratio, has a long clinical application history of more than 700 years in China. We found SGF effective in HF in our previous clinical studies, including ameliorating patients clinical symptoms,[13] strengthen cardiac systolic function,[14] and inhibiting brain natriuretic peptide or N-terminal pro B type natriuretic peptide.[15]

Another previous study indicated that Gu Ben Pei Yuan San, another TCM formula containing ginseng, gecko, and other herbs, could improve cardiac function and repair the myocardium in adult mice after apical resection or myocardial infarction.[16] In addition, the TCM Qishenkeli, which contains ginseng, has also been shown to play an anti-heart failure role by improving heart function and having anti-apoptosis properties.[17] However, whether SGF has a cardioprotective function has not been clarified, and the underlying mechanism has not been elucidated.

In this study, we investigated the effect of SGF on an HF model induced by abdominal aorta constriction (AAC) in rats and tested Akt, p53, HIF-1α, VEGF, Bax, bcl-2, and caspase-3 to explore the possible mechanisms involved.

Materials and Methods

Sample Preparation

Ginseng (lot #180702) was purchased from Shanghai Shangyao Shenxiang Health Pharmaceutical Co., Ltd, and gecko (lot #190812) was purchased from Shanghai Lei Yun Shang Pharmaceutical Co., Ltd, China. Chinese herbal medicine was identified by Longhua Hospital Professor Xin Zhou, according to the 2015 Pharmacopoeia of the People's Republic of China (Chinese Pharmacopoeia; Table 1). Ginseng was powdered using a pulverizer and then collected after No.10 filter selection. According to the Chinese Pharmacopoeia, the gecko was removed without squama, head, and paws and then collected using the same method as that used for ginseng. SGF powder mixture was then made up by mixing Ginseng powder and gecko powder with weight ratio of 3:1.

Table 1 Ingredients of SGF Used with English Translations

Latin Scientific Name	English Name Name	Herb Name Name	Herb Parts
Panax ginseng C.A.Mey.	Ginseng	Renshen	Roots and rhizomes
Gekko gecko Linnaeus	Gecko	Gejie	Body without squama, head, and paws

Abbreviation: SGF: Shen'ge formula.

Chemical Analysis of SGF

Chemical analysis of SGF was conducted using high-performance liquid chromatography (HPLC). Since most of the ingredients in geckos are trace elements and amino acids without characteristic components, we selected four major representative saponins in ginseng as reference substances. A quadrupole-electrostatic field orbitrap high-resolution mass spectrometry system (Q Exactive, Thermo Fisher, USA) and an ultra-performance liquid chromatography system (Dionex Ultimate 3000, Thermo Fisher, USA) were used for chemical analysis. SGF (0.10286 and 0.10591 g) was extracted with 5 mL methanol by ultrasound for 30 min. The concentrations of the SGF samples were 205.72 and 211.82 μg/mL. The reference substances (ginsenoside Rb1, Rb3, Rc, and Rd) were diluted with methanol to 1 μg/mL for the following detection. Chromatographic analysis was performed using a chromatographic column (ACQUITY UPLC HSS T3, 2.1 × 100 mm, 1.8 μm, Waters, USA) using 0.1% formic acid in aqueous solution (C) and acetonitrile (D) for gradient elution (0–1 min, 40% D; 1–4 min, 40–65% D; 4–6 min, 65–70% D; 6–7 min, 70% D; 7–8 min, 40% D; flow velocity, 0.3 mL/min; temperature, 45°C). Mass spectrum parameters were as follows: Ion Max Heated Electrospray spray voltage: +3.2KV/-2.8 KV; sheath gas pressure: 35arb; auxillary gas pressure: 10arb; capillary temperature: 320°C; heater temperature: 300°C; scan mode: Full MS (resolution 70,000); scan range: m/z 80–1200.

Reagents

Bisoprolol (BSP; lot # 07002070) was purchased from Merck Pharmaceutical Co., Ltd. Chromatographic methanol (lot # 196565) and grade acetonitrile (lot # 203025) were acquired from Thermo Fisher Scientific Inc. Ginsenoside Rb1 (lot# 110,704–202,028) was obtained from the China Institute for Food and Drug Control, while ginsenoside Rb3 (lot # 6108), ginsenoside Rc (lot # 3508), and ginsenoside Rd (lot # 5826) were purchased from Shanghai Nature Standard Technical Service Co., Ltd. Chloral hydrate (lot # FC25BA0008) was obtained from Sangon Biotech (Shanghai) Co., Ltd. Tissue RNA Purification Kit PLUS (lot # RN1P190906), 4 × EZscript Reverse Transcription Mix II (lot # R2GQ200309) and 2 × Color SYBR Green qPCR Master Mix (lot # A1R2191219) were acquired from ZScience Biotechnology Co., Ltd. Hoechst (lot # 022519191104) and fluorescence primary antibody (lot # 329C031) were obtained from Beyotime Technology Co., Ltd. VEGFR2 (lot # 4), α-SMA (lot # 3), GAPDH (lot # 14), PCNA (lot # 14), p-p53 (lot # 21), p53 (lot # 15), p-Akt (lot # 14), Akt (lot # 28), HIF-1α (lot # 3), anti-rabbit (lot # 29) and anti-mouse (lot # 35) were all purchased from Cell Signaling Technology Inc.

Experimental Animals and Protocols

Male Wistar rats (weight: 180–200g) were purchased from Vital River (Shanghai, China, No. 11100111911058728). All animals were housed in specific pathogen-free (SPF) conditions under a 12 h light/dark cycle with a temperature of 23 ± 3°C and a relative humidity of approximately 50%. The HF model was established by partial AAC according to an established procedure.[18,19] Briefly, rats were anesthetized with 3% pentobarbital sodium (40 mg/kg) via intraperitoneal injection, and the abdominal aorta was partially ligated by a 6–0 suture banded between the two renal arteries over a 23-gauge needle. Needle was removed immediately after the surgery. This experimental protocol was approved by the Animal Research Ethics Committee of Shanghai University of TCM (Approval no.: PZSHUTCM191108013). All the animal care and experimental procedures follow the Guidelines for the Care and Use of Laboratory Animals developed by the Ministry of Science and Technology of China, and the Animal Research Ethics Committee of Shanghai University of TCM, and all methods are reported in accordance with ARRIVE guidelines for the reporting of animal experiments. As 3g/day clinical use of SGF in one adult, rats in SGF group were treated with SGF 1.89g/kg day through intragastric

administration according to experimental methodology of pharmacology[20] and our previous study.[21] Bisoprolol was intragastrically administrated 1 mg/kg day.[22,23]

Echocardiography

Transthoracic echocardiography was performed using a small animal B ultrasound instrument (VisualSonics, Canada) after anesthesia with pentobarbital sodium at 8 and 24 weeks of treatment. All measurements were presented as the mean of three consecutive cardiac cycles. The left ventricular ejection fraction (EF), fractional shortening (FS), left ventricular internal diameter (LVID), interventricular septum (IVS), and left ventricular volume (LVVOL) were measured using computer algorithms by a 20MHz transducer probe from the long-axis view. After echocardiography, rat heart tissues were preserved in liquid nitrogen and paraformaldehyde.

Hematoxylin-Eosin and Immunofluorescent Staining

After ultrasonic examination, the heart was separated and removed without the major vessels, atria, or right ventricle. The heart was fixed in 4% paraformaldehyde, embedded in paraffin, and stained with hematoxylin and eosin (HE) and immunofluorescence to evaluate cardiac status. Pictures were acquired by microscopy, and seven fields of each section were captured. The cardiomyocyte cross-sectional area was measured by software ImageJ.[24] VEGFR2 and α-SMA were observed by immunofluorescence staining to measure the degree of myocardial angiogenesis in cardiac myocytes. In brief, after dewaxing and rehydration of myocardial tissue, antigen repair was performed, and non-immune serum was closed, followed by 12 h fluorescence primary antibody diluent with α-SMA or VEGFR2 (1:400) at 4°C and secondary antibody for another 1.5 h at 25°C. Hoechst was used to stain the nuclei, and the slices were sealed. Images were observed and taken under a fluorescence microscope, and seven fields of each section were captured.

TUNEL Assay

The heart sections were fixed in 4% paraformaldehyde (Beyotime, China) and were incubated with 50 μL TUNEL reaction mixture (Promega, USA) and 0.3% Triton X-100 in the dark (37 °C) for 1 h. After washing three times with PBS, Nuclei were labelled with the DAPI (Beyotime, China) after 5 min. The heart sections were then observed under a confocal microscope (Leica, Germany) under each experimental condition.

Quantitative Real-Time Polymerase Chain Reaction

Total RNA was isolated using an EZBioscience reagent and reverse transcribed into cDNA. Quantitative real-time polymerase chain reaction (qPCR) was performed under the following conditions: 95°C for 10 min, followed by 40 cycles at 95°C for 10s and 60°C for 30s. β-actin was used as an internal reference and the $2^{-\Delta\Delta CT}$ method was employed to analyze the relative results. The primers are described in Table 2.

Western Blot Analysis

The heart tissues were cut into small fragments. A total of 100 μL of lysate were added to 10 mg of each tissue, and tissues were homogenized until completely lysed. The supernatant was collected after centrifugation (10,000 g for 5 min at 4°C). The proteins were then extracted, separated, and transferred onto polyvinylidene difluoride membranes, blocked with 5% nonfat milk overnight at 4°C. The blots were incubated with antibodies (1:1000) to p-p53, p53, p-Akt, Akt, HIF-1α, and VEGFR2, and then with secondary antibody (1:2000; anti-rabbit and anti-mouse at 25°C for 1 h). Grayscale scanning analysis was performed using an electrochemiluminescence (ECL) detection kit to determine protein content. GAPDH (glyceraldehyde-3-phosphate dehydrogenase) was used as an internal reference for total cell and cytoplasmic proteins, while PCNA (proliferating cell nuclear antigen) was used as a nuclear protein.

Statistical Analysis

All analyses were performed using SPSS 25.0. Data are expressed as mean ± standard deviation (SD) when normally distributed, while the median (interquartile spacing) is used for non-normal distribution. Differences among groups were

Table 2 Forward and Reverse Primer Sequences for qPCR

Gene	Forward Primer	Reverse Primer
α-MHC	TCCAAGGGCATCTTCCTAGA	CAGGCAAAGTCAAGCATTCA
β-MHC	TCAAGCTGGAGCAGCAAGT	TCATCCAACTGCTGCTTGTC
VEGF	GCCCTGAGTCAAGAGGACAG	CAGGCTCCTGATTCTTCCAG
HIF-1α	TCAAGTCAGCAACGTGGAAG	TATCGAGGCTGTGTCGACTG
Caspase3	TCCTTCAGTGGTGGACATGA	TCAACAATTTGAGGCTGCTG
p53	GTCTACGTCCCGCCATAAAA	AGGCAGTGAAGGGACTAGCA
Bax	CGAGCTGATCAGAACCATCA	CTCAGCCCATCTTCTTCCAG
Bcl-2	GGGATGCCTTTGTGGAACTA	CTCACTTGTGGCCCAGGTAT
β-Actin	ATGACGATATCGCTGCGCTC	CCCATACCCACCATCACACC

analyzed using one-way analysis of variance (ANOVA), and the least significant difference (LSD) test was performed between groups. Statistical significance was set at $p < 0.05$.

Results

Chemical Identification and Content Determination of SGF

Figure 1 presents the HPLC chromatogram alongside the chemical structure of SGF. Ginsenosides Rb1, Rb3, Rc, and Rd exhibited retention times of 2.55, 3.19, 2.89, and 3.79 min, respectively. In SGF, the concentrations of ginsenoside Rb1, Rb3, Rc, and Rd were measured at 17.58, 6.01, 6.02, and 1.94 ng/g, correspondingly. Notably, ginsenoside Rb1 emerged as the predominant chemical component within SGF, surpassing the quantities of the other constituents.

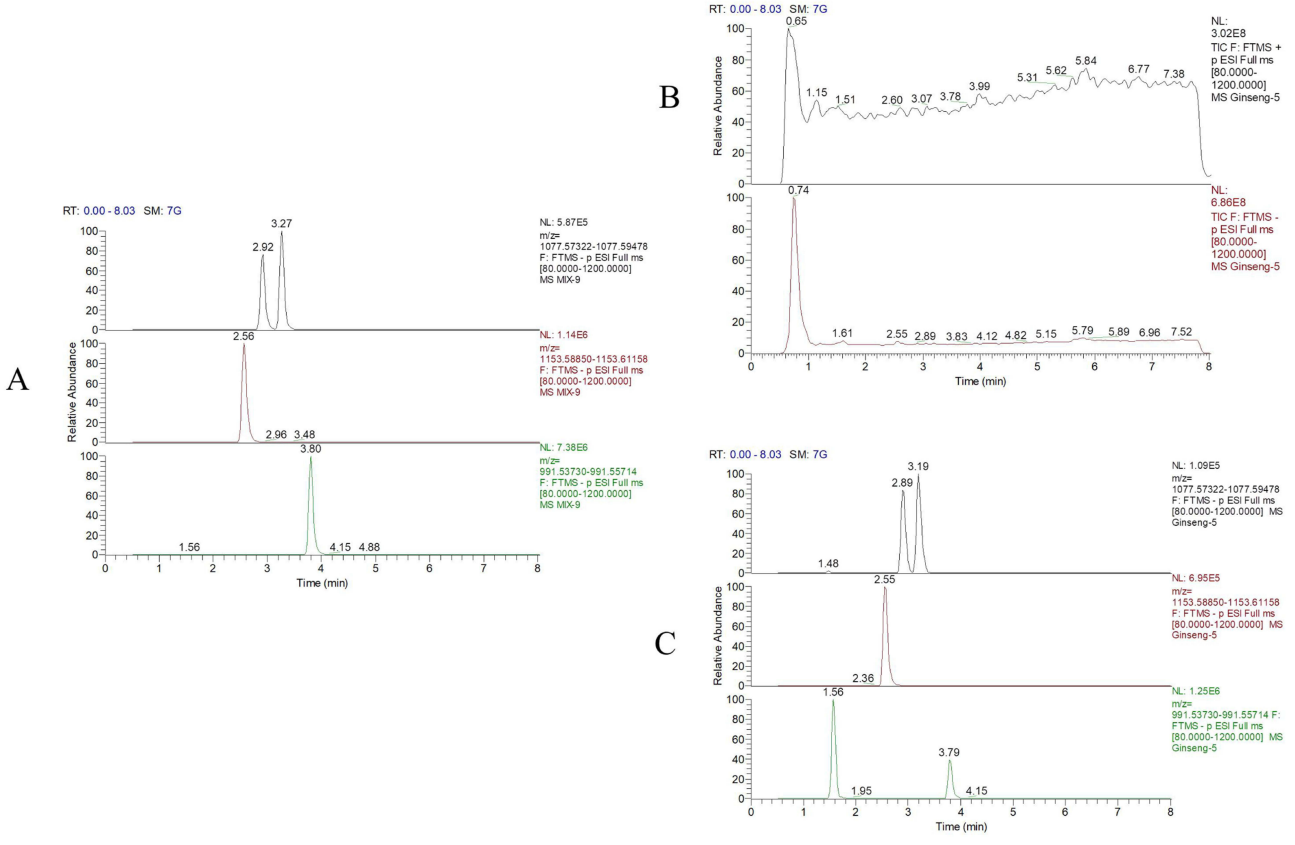

Figure 1 Chromatograms of reference substances (**A**), the total ion chromatograms of SGF (**B**), and chromatograms of reference substances in SGF (**C**). The retention times in (**A**) were: 2.56 min, ginsenoside Rb1; 3.27 min, ginsenoside Rb3; 2.92 min, ginsenoside Rc; 3.80 min, ginsenoside Rd. The retention times in (**C**) were: 2.55 min, ginsenoside Rb1; 3.19 min, ginsenoside Rb3; 2.89 min, ginsenoside Rc; 3.79 min, ginsenoside Rd. SGF, Shen'ge formula.

SGF Improves Pressure Overload-Induced Ventricular Remodeling

SGF Ameliorates Cardiac Function

To investigate the impact of SGF on ventricular remodeling induced by pressure overload, AAC surgery was conducted, with cardiac function assessed via echocardiography (Figure 2A and B). At 8- and 24-weeks post-gavage, AAC rats showed a noticeable deterioration of heart function and cardiac structural change, indicated by decreased EF, FS, and IVS and increased LVID and LVVOL during systole (s) and diastole (d). Compared with the AAC group, treatment with SGF and BSP improved EF and FS and reduced LVIDs, LVIDd, LVVOLs, and LVVOLd ($p < 0.05$). Additionally, while IVS was diminished in the AAC group, it showed improvement following SGF or BSP administration (Figure 2C–J and K–R).

SGF Inhibits Cardiac Hypertrophy

The Heart Weight/Body Weight ratio (HW/BW) and HE staining were then used to assess cardiac hypertrophy. HW/BW, calculated at 24 weeks post oral gavage, increased obviously in AAC group, comparing with Sham group but decreased significantly in SGF group, compared to AAC group ($p < 0.05$, Table 3).

Heart tissue samples for HE staining were selected at 8 and 24 weeks post oral gavage. HE staining results showed that, compared with Sham group, myocardial fibers in the AAC group were disordered, the myocardial intercellular space was enlarged, and the transverse diameter of the myocardium increased. SGF usage apparently resulted in the alleviation of these pathologic alterations (Figure 3A–F).

SGF Promotes Angiogenesis in Heart Failure

As heart function worsened at 24 weeks post-gavage, immunofluorescent staining was used to assess the function of SGF in myocardial angiogenesis in HF rats. Rat myocardial nuclei were stained blue by Hoechst staining, while α-SMA and VEGFR2 were highlighted green by fluorescence. Quantitative fluorescence results showed that, compared with Sham group, α-SMA was significantly increased ($p < 0.001$), while VEGFR2 was significantly decreased in the AAC group ($p < 0.001$), which significantly improved after the intervention with SGF and BSP ($p < 0.05$; Figure 4A–D). These results indicated that SGF inhibited α-SMA and promoted VEGFR2 expression in AAC rats.

SGF Downregulates the Expression of Apoptosis-Associated Molecules and Improves anti-HF-Associated Molecules

Given the observed improvements in heart function and the inhibition of cardiac hypertrophy afforded by SGF, we further explored its influence on the mRNA expression of heart failure (HF)-related molecules, including *α-MHC, β-MHC, p53, Caspase*-3, *Bax, Bcl-2, VEGF*, and *HIF-1α*, at 8 (Figure 5A–H) and 24 weeks (Figure 5I–P) post-gavage. At the 8-week mark, the AAC group exhibited significantly elevated mRNA levels of *α-MHC, β-MHC, HIF-1α, Caspase-3*, and *Bcl-2* compared to the sham group. These increases were notably reduced following the administration of SGF. Similarly, eight weeks after gavage, the apoptosis was significantly higher in the AAC group than sham group through TUNEL assay; however, SGF effectively reduced the apoptosis (Supplementary Figure 1A and 1B). VEGF levels were significantly higher in SGF than in AAC, and *p53* was higher in the AAC group than sham group, but it was not significantly downregulated by SGF. Further analysis showed that after 24 weeks of gavage, there were new changes in the expression of molecular mRNA. The mRNA levels of *α-MHC*, HIF-1α, *VEGF*, and *Bcl-2* were significantly higher in SGF than in AAC, while mRNA levels of *β-MHC, p53, Caspase-3*, and *Bax* were significantly lower in SGF than in AAC.

SGF Upregulates Akt, HIF-1α and Inhibits p53

To further identify underlying mechanism of SGF in HF-associated molecule modulation, we detected total protein levels of p-Akt, Akt, p-p53, p53 and HIF-1α at 8 (Figure 6A–F) and 24 weeks (Figure 6G–L) post-surgery and cytoplasmic (Figure 6M–O), nuclear (Figure 6P–R) protein levels of p53, and HIF-1α were also detected at 24 weeks post-surgery. Data showed that, at both 8- and 24-weeks post-gavage, p-Akt, Akt, and HIF-1α decreased obviously in AAC group and distinctly increased in SGF group. p-p53 and p53 both increased following AAC, which was significantly inhibited by SGF ($p < 0.01$; Figure 6A–L). Results of cytoplasmic protein detection showed that, compared to AAC group, SGF apparently reduced p53 level ($p < 0.05$). Although the trend that SGF increased HIF-1α in cytoplasm compared to AAC

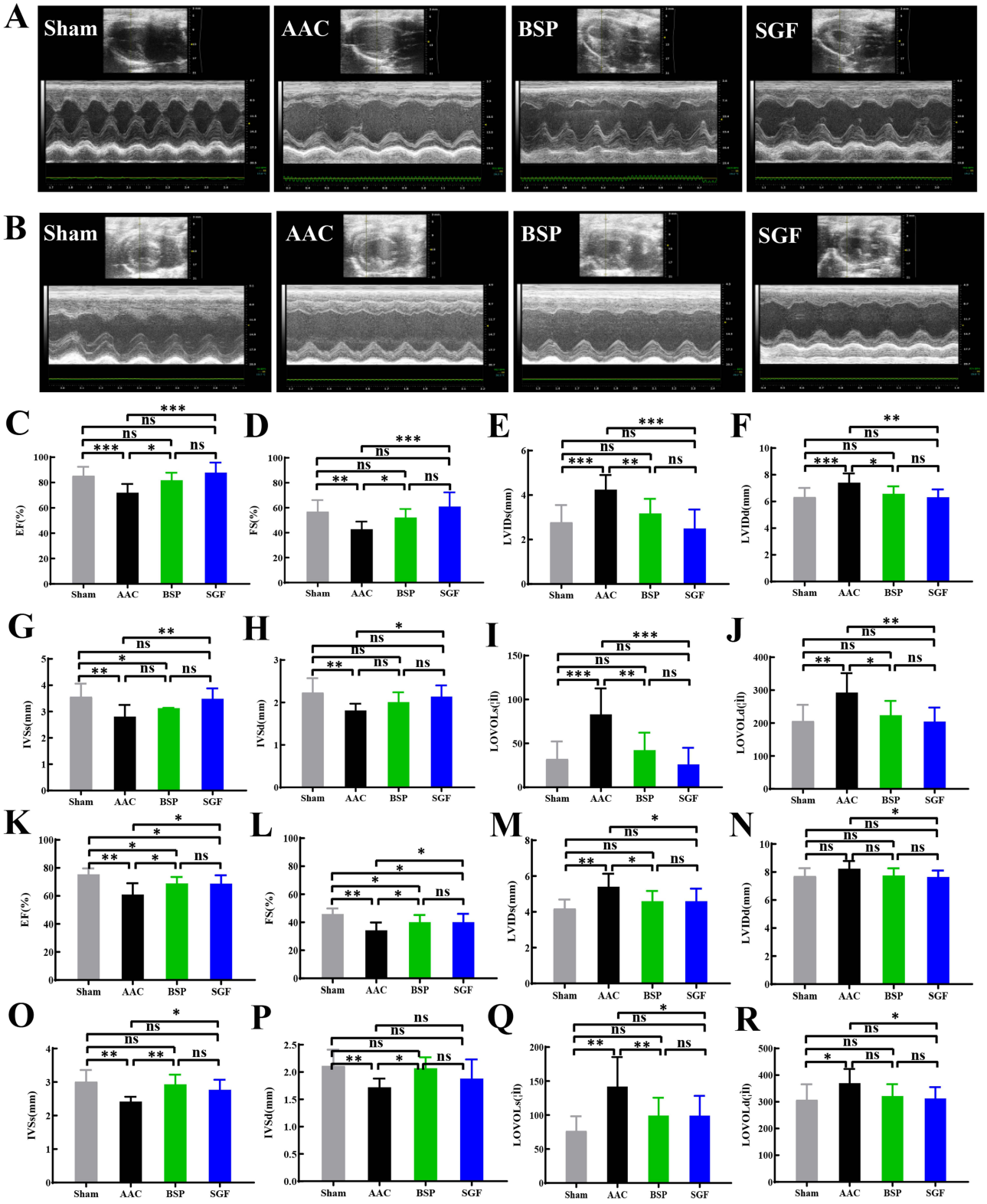

Figure 2 SGF protects rat heart function and cardiac remodeling after AAC. Echocardiography of pressure overload-induced HF rats after 8 (**A**) and 24 weeks (**B**) oral gavage. (**C**–**J**) and (**K**–**R**) were the corresponding results of A and B, following EF, FS, LVID, IVS, and LVVOL in each group. ns $p > 0.05$; * $p < 0.05$, ** $p < 0.01$; *** $p < 0.001$. Data are presented as mean ± standard deviation and were collected from 10 rat in Sham group, 8 rat in AAC group, 7 rat in BSP group, 7 rat in SGF group after 8 weeks oral gavage and 9 rat in Sham group, 7 rat in AAC group, 9 rat in BSP group, 7 rat in SGF group after 24 weeks oral gavage.

Abbreviations: SGF, Shen'ge formula; AAC, abdominal aortic constriction; BSP, bisoprolol; HF, heart failure; EF, left ventricular ejection fraction, FS, fractional shortening; LVID, left ventricular internal diameter; IVS, interventricular septum; LVVOL, left ventricular volume.

https://doi.org/10.2147/DDDT.S451720 DovePress

Table 3 Tissue Characteristics of Rats After 24 Weeks of Oral Gavage

	Heart Weight (mg)	Body Weight (g)	HW/BW (mg/g)
Sham	1485.71±55.03	617.00±21.95	2.41±0.06
AAC	1492.86±93.76	559.43±32.82**	2.68±0.27*
BSP	1470.00±124.10	594.43±33.00	2.47±0.17
SGF	1390.00±128.19	572.17±45.73*	2.44±0.22#

Notes: Data are presented as mean ± standard deviation and collected from 9 rat in Sham group, 7 rat in AAC group, 9 rat in BSP group, 7 rat in SGF group. SGF, Shen'ge formula; AAC, abdominal aortic constriction; BSP, bisoprolol; HW, Heart Weight; BW, Body Weight. *$p < 0.05$ and **$p < 0.01$ compared to Sham, #$p < 0.05$ compared to AAC.

group, no significance existed in HIF-1α between AAC and SGF group (Figure 6M–O). The detection of nuclear protein showed that SGF evidently increased HIF-1α level ($p < 0.05$) and reduced p53 level in nucleus ($p < 0.001$; Figure 6P–R). These results demonstrate that SGF could promote HIF-1α and inhibit p53 transportation into nucleus probably by upregulating and phosphorylating Akt in pressure-overload HF induced by AAC.

Discussion

Long-term myocardial damage and cardiac overload lead to decrease cardiac contractility. Ventricular remodeling with myocardial hypertrophy and apoptosis is a typical pathological feature of the development of HF. In this study, we explored pressure overload-induced heart failure (HF) using abdominal aorta constriction (AAC) models in rats. The AAC rats exhibited clear indications of HF progression, including diminished cardiac function, myocardial hypertrophy, and increased apoptosis. This model is extensively utilized for investigating pharmacological interventions in cardiac remodeling associated with heart dysfunction and hypertrophy.[25,26] Chinese herbal medicines (CHM), which are beneficial for HF patients and beneficial for their life quality,[27] have been used in various heart diseases in China for thousands of years. CHM is offered as a complementary or alternative treatment for primary and secondary prevention of heart diseases.[28] SGF, as one kind of CHM, is composed of

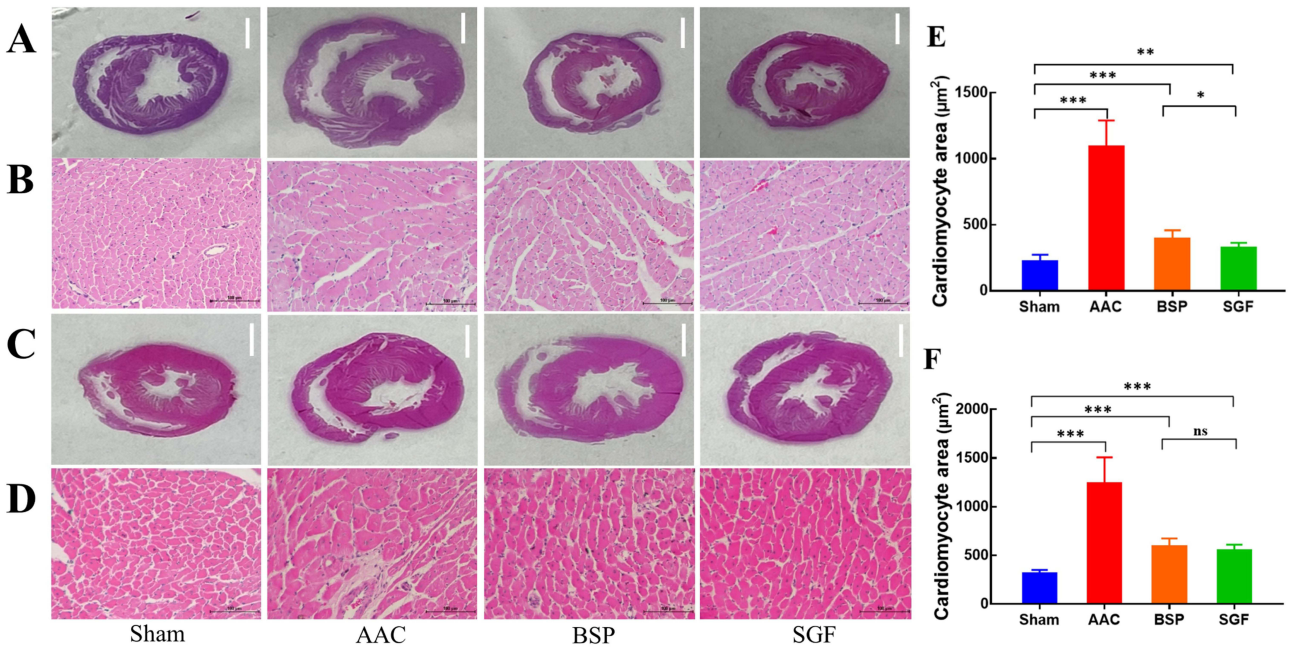

Figure 3 HE staining of cardiac tissue. (**A**) is the rat heart section after 8 weeks of gavage, (**B**) is the corresponding enlarged images, (**C**) is the section after 24 weeks of gavage, and (**D**) the corresponding enlarged images. (**E**) is cardiomyocyte cross sectional area after 8 weeks of gavage. (**F**) is cardiomyocyte cross sectional area after 24 weeks of gavage. The white ruler in (**A**) and (**C**) is 2mm, and the black ruler in (**B**) and (**D**) is 100 μm. ns $p > 0.05$; * $p < 0.05$, ** $p < 0.01$; *** $p < 0.001$. Data are presented as mean ± standard deviation (n = 5 for HE staining, n = 25 for myocyte cross sectional area).
Abbreviations: HE, hematoxylin and eosin; SGF, Shen'ge formula; AAC, abdominal aortic constriction; BSP, bisoprolol.

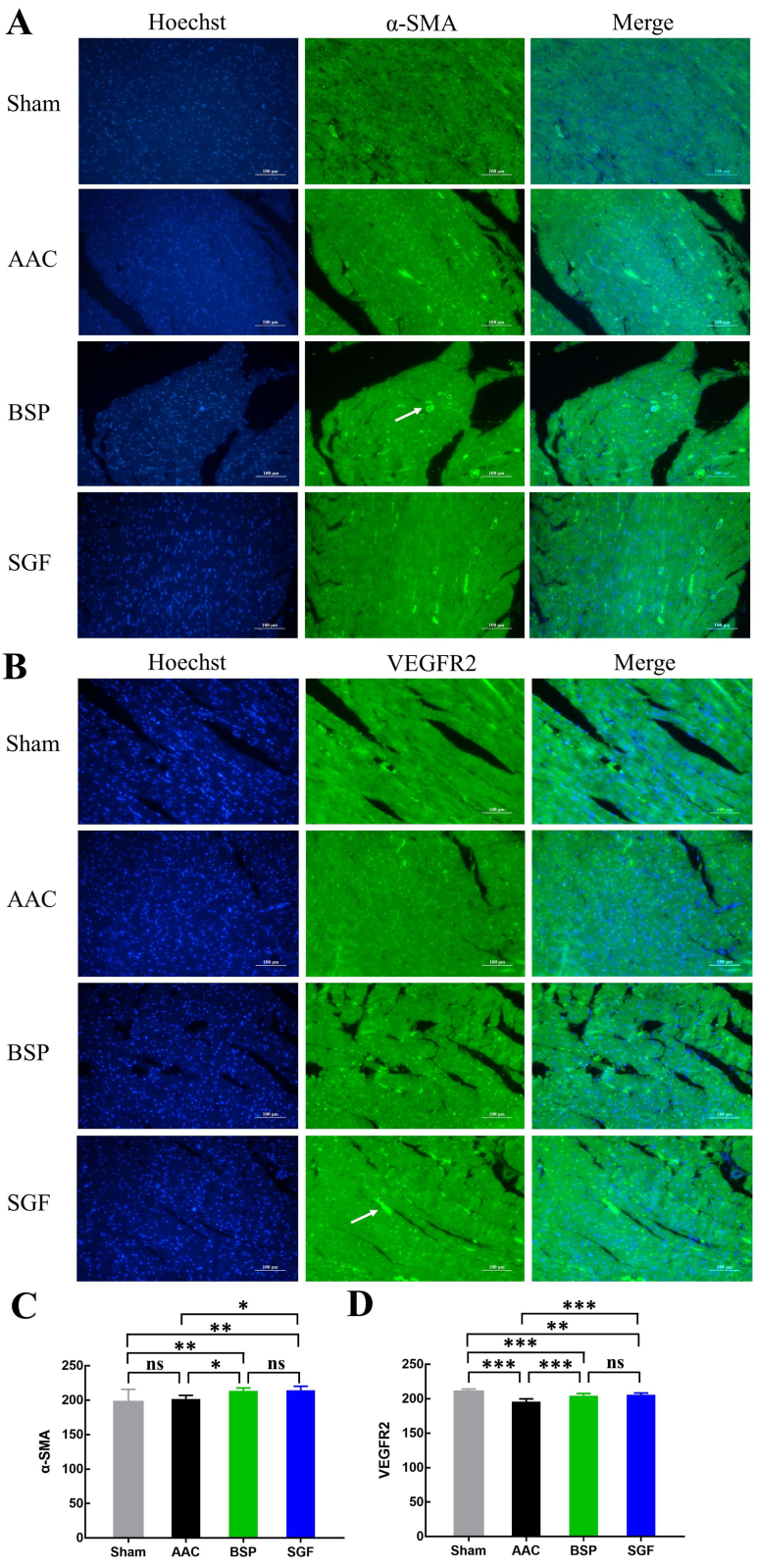

Figure 4 Immunohistochemical detection of α-SMA and VEGFR2 expression. The bright blue spot is the nucleus stained by Hoechst, and the highlighted green pointed by the white arrow is the expression of α-SMA (**A**) or VEGFR2 (**B**). (**C**) and (**D**) are the semi-quantitative fluorescence analysis results corresponding to (**A**) and (**B**) by ImageJ. The scale is 100μm. ns $p > 0.05$; * $p < 0.05$; ** $p < 0.01$; *** $p < 0.001$. Data are presented as mean ± standard deviation (n = 5).
Abbreviations: SGF, Shen'ge formula; AAC, abdominal aortic constriction; BSP, bisoprolol.

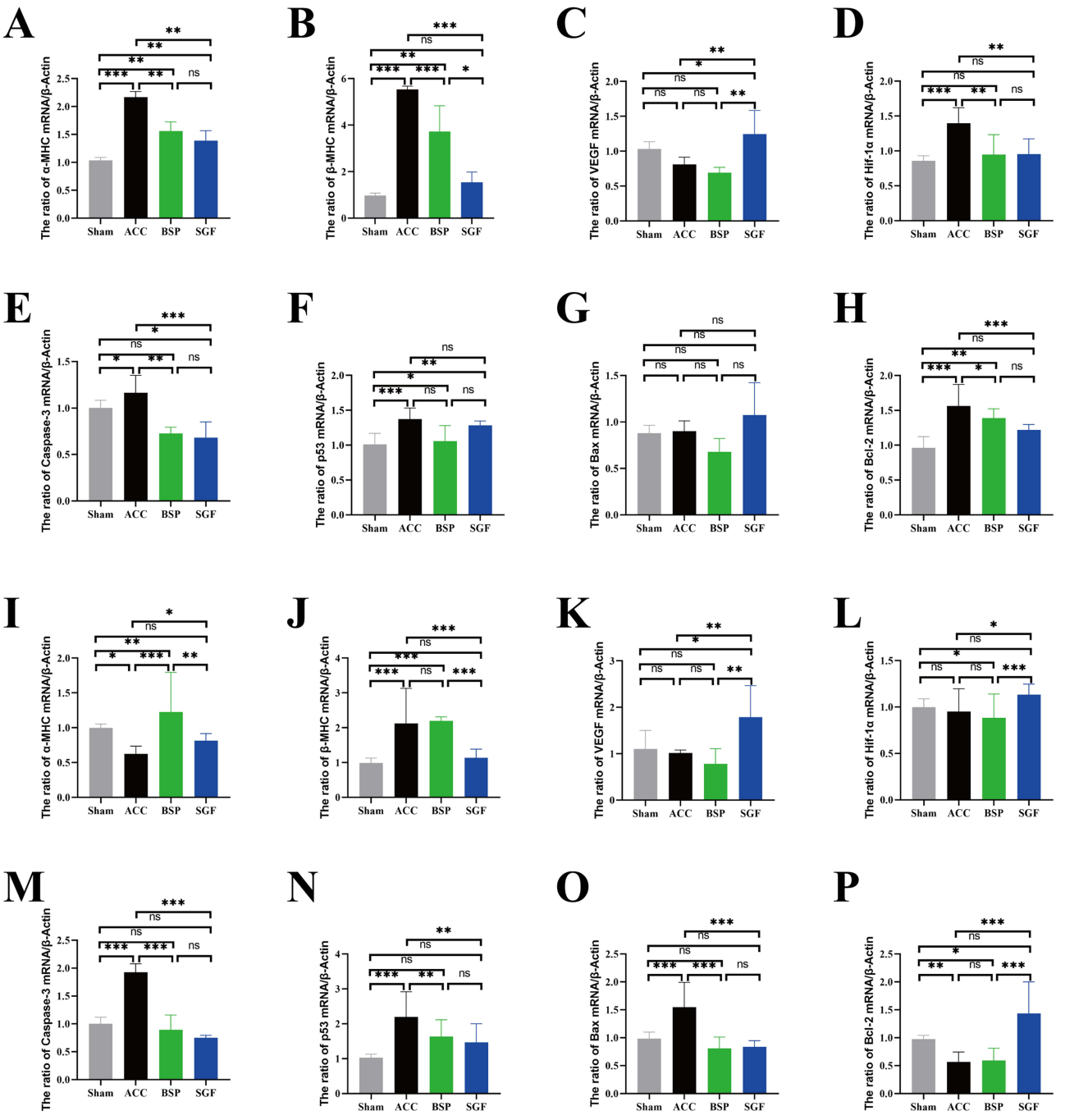

Figure 5 The expression of *α-MHC, β-MHC*, VEGF, HIF-1α, Caspase-3, p53, Bax, and Bcl-2 was analyzed by performing qPCR after 8 (**A**–**H**) and 24 weeks (**I**–**P**) of oral gavage. ns $p > 0.05$; * $p < 0.05$; ** $p < 0.01$; *** $p < 0.001$. mRNA expression data were normalized with the reference mRNA expression, β-Actin. Data are presented as mean ± standard deviation (n = 5).

Abbreviations: qPCR, quantitative real-time polymerase chain reaction; SGF, Shen'ge formula; AAC, abdominal aortic constriction; BSP, bisoprolol.

ginseng and gecko. Ginseng is the root of Panax ginseng, which has a long history of medical use in Asia. It is increasingly used in health maintenance and cardiovascular disease treatment in the United States,[29] Canada,[30] and Europe.[31] Presently, there are few studies available on the modern pharmacology of geckos. In the Chinese Pharmacopoeia, geckos are reported to nourish the lungs and kidneys, absorb qi, relieve asthma, and exert symptomatic effects on chest tightness and shortness of breath caused by cardiac insufficiency.

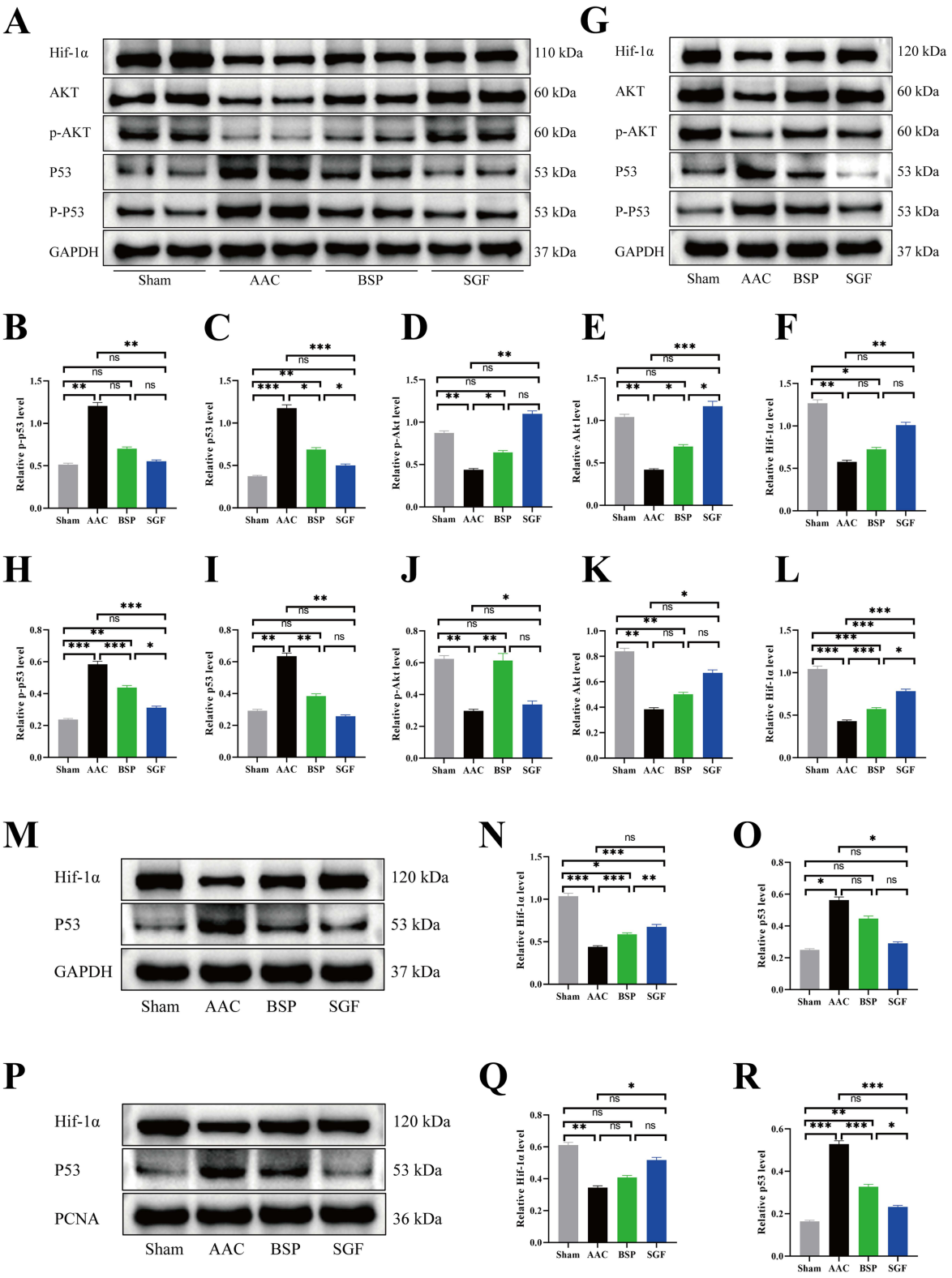

Figure 6 SGF upregulates Akt, HIF-1α and inhibits p53 protein expression. The total protein levels of p-Akt, Akt, p-p53, p53, and HIF-1α in each group are shown at 8 (**A**–**F**) and 24 weeks (**G**–**L**) post-gavage. The protein levels of HIF-1α and p53 in the cytoplasm (**M**–**O**) and nucleus (**P**–**R**) are shown at 24 weeks post-gavage. Quantitative analysis of the bands was calculated by ImageJ. ns $p > 0.05$; * $p < 0.05$; ** $p < 0.01$; ***$p < 0.001$. Data are presented as mean ± standard deviation (n = 5). **Abbreviations**: SGF, Shen'ge formula; AAC, abdominal aortic constriction; BSP, bisoprolol.

https://doi.org/10.2147/DDDT.S451720 DovePress

Considering the complex composition of herbs, we identified extracts in SGF using the Q Exactive analysis system. Given that the primary constituents of geckos are trace elements and amino acids, lacking distinctive components, analyzing their composition holds limited value. Chemical profile and quality control methods of SGF were established by content detection of several chemical standards, including ginsenoside Rb1, Rb3, Rc, and Rd. These constituents were considered active components of SGF, and the amount of ginsenoside Rb1 was significantly higher than that of the other compounds. The administration of ginsenoside Rb1 improves cardiac function and remodeling following abdominal aortic coarctation.[32] In a high-load-induced model of HF in rats, ginsenoside Rb1 exhibits a cardioprotective role by inhibiting myocardial autophagy through the Rho/ROCK and PI3K/mTOR pathways.[33] Ginsenoside Rb3[34] has been found to protective benefits against isoproterenol-induced heart impairment in rats. The impacts of other components found in ginseng and gecko on heart health are still to be determined. This underscores the need for further research into the cardioprotective elements present in SGF to fully understand their potential benefits.

In this research, BSP, a beta-blocker endorsed for heart failure (HF) treatment, served as the positive control against which SGF's effects were compared. Numerous extensive trials involving HF patients have confirmed that oral administration of beta-blockers can significantly reduce all-cause mortality and enhance both symptoms and quality of life.[35,36] Moreover, beta-blockers improve cardiac muscle performance in patients with HF.[37] Our research shown that SGF exerted an effect on cardiac function similar to that by BSP. Both BSP and SGF elevated EF and FS and alleviated LVID and LVVOL. These results suggested that SGF could protect the structure and function of heart. Moreover, SGF not only improved heart function but also inhibited myocardial hypertrophy. AAC-induced pressure overload would lead to cardiomyocyte hypertrophy and myocardial thickening, which ultimately progress to HF.[38] *β-MHC*, one molecular marker of cardiac hypertrophy, was markedly increased in AAC group, but significantly attenuated by SGF. Additionally, HE staining also showed that SGF obviously reduced cardiac myocyte cross-sectional area. Consequently, SGF could reduce cardiac hypertrophy.

Hypertrophic hearts have been reported to have inhibited angiogenesis and endothelial dysfunction.[39,40] The pathological overload of the myocardium leads to the hypertrophic response, which increases the oxygen consumption of the myocardium and induces angiogenesis to maintain cardiac pump function in the hypoxic state. Consequently, a beneficial approach to treating heart failure involves the use of medications that both counteract hypertrophy and promote angiogenesis.[9] During myocardial ischemia and hypoxia, activation of HIF-1α can be mediated by vascular remodeling,[41] and *VEGF* positively contributes to the maintenance of angiogenesis.[42] We then examined the expression of *VEGF, VEGFR2*, and *HIF-1α* to further clarify the pro-angiogenesis effect of SGF in HF rats. Molecular detection demonstrated that SGF could upregulate *VEGF* and *HIF-1α* in rats with pressure overload. Immunofluorescence manifests that expression of *VEGFR2* and *α-SMA*, which was often used to label myocardial microvessel,[43,44] was both increased in cardiac muscle tissue after using BSP and SGF. Therefore, we concluded that SGF provided cardioprotection to HF also by increasing myocardial angiogenesis.

In addition to cardiac hypertrophy and angiogenesis, cardiomyocyte apoptosis is considered the key factor for the progression of HF from compensation to decompensation. Accordingly, to identify potential therapeutic targets of SGF for apoptosis, Akt and p53 were detected by Western blotting, and the relevant apoptotic genes were detected by qPCR. PI3K/Akt signaling pathway actively participates in and mediates the apoptosis process,[45] by regulating various apoptotic factors, such as *Caspase-3, Bax, Bcl-2, p53*, and other apoptotic factors.[46,47] As apoptosis is an orderly regulated process, early intervention may effectively block the apoptosis process.[48] In this study, we found that SGF markedly upregulated and phosphorylated *Akt* and reduced *p53* in AAC-induced HF. Additionally, SGF and BSP apparently downregulated *p53, caspase-3, Bax*, and upregulated *Bcl-2* levels. This indicated that SGF could downregulate apoptosis-related factors in pressure overload HF.

Mechanistically, both *HIF-1α* and *p53* are involved in the hypoxic cell response and interact with each other.[49] In moderate hypoxia, *HIF-1α* activation promotes vascular growth and protein phosphatase 1 nuclear-targeting subunit induced *p53* accumulation, promoting apoptosis and Mdm2-dependent degradation of *HIF-1α*.[50,51] To further clarify the role of SGF, we detected the expression of *HIF-1α* and *p53* in the cytoplasm and nucleus. Although SGF effected no significance on cytoplasmic *HIF-1α* expression, it significantly enhanced nuclear *HIF-1α* expression. Meanwhile, SGF reduced nuclear and cytoplasmic *p53* levels, which were more prominent in nucleus. These data indicated that SGF plays

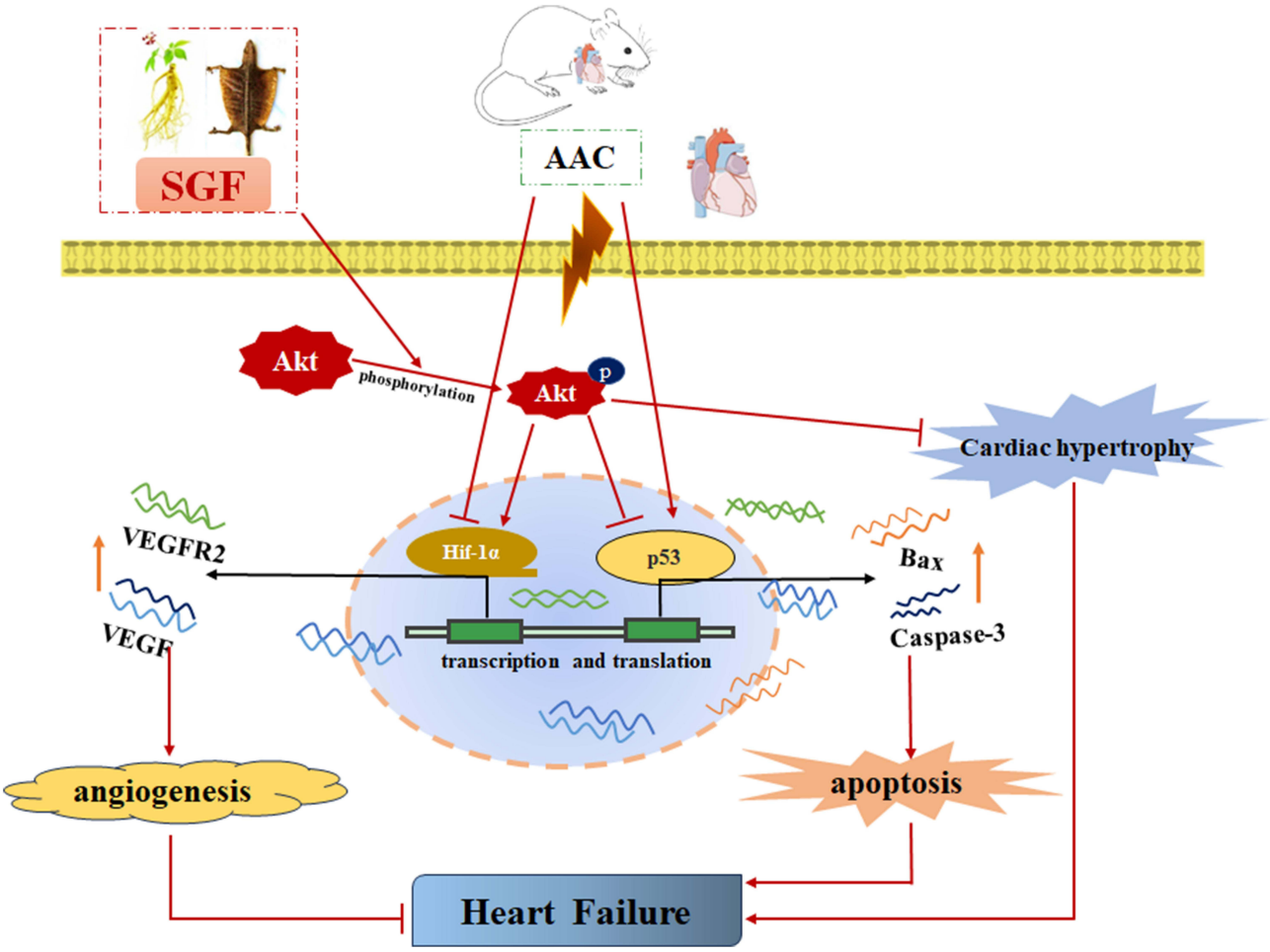

Figure 7 Mechanistic diagram of SGF in preserving cardiac function against AAC-induced heart failure. SGF, Shen'ge formula; AAC, abdominal aortic constriction.

a cardioprotective role probably by promoting *HIF-1α* and inhibiting *p53* transport to the nucleus. Thus, comprehensively, SGF exerts cardioprotective effect, including anti-hypertrophy, anti-apoptosis, and pro-angiogenesis, by upregulating and phosphorylating *Akt*, which then facilitating *HIF-1α* nucleus transportation and inhibiting *p53* nucleus transportation (Figure 7).

Conclusion

In conclusion, our study investigated the protective effects of SGF in an animal model of HF and might provide a new strategy for the treatment of HF. We confirmed that SGF could prevent ventricular remodeling by inhibiting cardiac hypertrophy and apoptosis and promoting angiogenesis. In addition, our findings demonstrated that SGF might confer protection against pressure overload-induced HF through the Akt/HIF-1α/p53 signaling pathway, which is involved in promoting HIF-1α and inhibiting p53 transport to the nucleus. The observed benefits could stem from the synergistic combination of diverse chemical constituents in SGF. Being a TCM formulation with multiple components, SGF has the potential to offer enhanced synergy across various targets to curb ventricular remodeling. This aspect merits deeper exploration. Future research should concentrate on identifying the active ingredients within SGF and assessing their potential for synergistic interactions.

Abbreviations

AAC, abdominal aortic constriction; BSP, Bisoprolol; SGF, Shen'ge formula; SPF, specific pathogen-free; HF, heart failure; HPLC, high-performance liquid chromatography; TCM, traditional Chinese medicine; EF, ejection fraction; FS, fractional

shortening; LVID, left ventricular internal diameter; IVS, interventricular septum; LVVOL, left ventricular volume; HE, hematoxylin and eosin; qPCR, quantitative real-time polymerase chain reaction; ECL, electrochemiluminescence; GAPDH, glyceraldehyde-3-phosphate dehydrogenase; PCNA, proliferating cell nuclear antigen; SD, standard deviation; ANOVA, analysis of variance; LSD, least significant difference; CHM, Chinese herbal medicines.

Data Sharing Statement

The original contributions presented in the study are included in the article. Further inquiries can be directed to the corresponding authors.

Ethics Approval and Consent to Participate

The authors are accountable for all aspects of the work in ensuring that questions related to the accuracy or integrity of any part of the work are appropriately investigated and resolved. This experimental protocol was approved by the Animal Research Ethics Committee of Shanghai University of TCM (Approval no.: PZSHUTCM191108013). All the animal care and experimental procedures follow the Guidelines for the Care and Use of Laboratory Animals developed by the Ministry of Science and Technology of China, and the Animal Research Ethics Committee of Shanghai University of TCM, and all methods are reported in accordance with ARRIVE guidelines for the reporting of animal experiments.

Acknowledgments

We are grateful to Tao Yang (Shuguang Hospital affiliated to Shanghai University of Traditional Chinese Medicine) for providing mass spectrometry services for Chinese herbs. We also thank the Animal Experiment Center of Shanghai University of TCM for echocardiographic services. The authors gratefully acknowledge all the experts of Central Laboratory of Longhua Hospital affiliated with Shanghai University of Traditional Chinese Medicine. We would like to thank Editage for English language editing.

Author Contributions

B.Q. and S.Q. contributed equally to this study. Corresponding authors D.Z. and Y.W. provided guidance. All authors made a significant contribution to the work reported, whether that is in the conception, study design, execution, acquisition of data, analysis and interpretation, or in all these areas; took part in drafting, revising or critically reviewing the article; gave final approval of the version to be published; have agreed on the journal to which the article has been submitted; and agree to be accountable for all aspects of the work.

Funding

This work was financially supported by the National Natural Science Foundation of China (81804010), Henan Provincial Health Commission national clinical research base of Traditional Chinese medicine (2022JDZX117); Henan Province Traditional Chinese medicine “double first-class” to create a scientific research project (HSRP-DFCTCM-2023-7-17).

Disclosure

The authors declare that the research was conducted in the absence of any commercial or financial relationships that could be construed as a potential conflict of interest.

References

1. Virani A SS, Alonso EJ, Benjamin MS, et al. Stroke statistics, heart disease and stroke statistics-2020 update: a report from the American Heart association. *Circulation*. 2020;141:e139–e596. doi:10.1161/CIR.0000000000000757
2. Maggioni AP, Dahlstrom U, Filippatos G, et al. Heart failure association of the European Society of, EURObservational research programme: regional differences and 1-year follow-up results of the heart failure pilot survey (ESC-HF Pilot). *Europ J Heart Fail*. 2013;15:808–817. doi:10.1093/eurjhf/hft050
3. Hao G, Wang X, Chen Z, et al. China Hypertension Survey, Prevalence of heart failure and left ventricular dysfunction in China: the China hypertension survey, 2012-2015. *Europ J Heart Fail*. 2019;21:1329–1337. doi:10.1002/ejhf.1629
4. Shimizu I, Minamino T. Physiological and pathological cardiac hypertrophy. *J Mol Cell Cardiol*. 2016;97:245–262. doi:10.1016/j.yjmcc.2016.06.001

5. Fan J, Li H, Nie X, et al. MiR-665 aggravates heart failure via suppressing CD34-mediated coronary microvessel angiogenesis. *Aging*. 2018;10:2459–2479. doi:10.18632/aging.101562
6. Chen S, Zhang Y, Lighthouse JK, et al. A novel role of cyclic nucleotide phosphodiesterase 10a in pathological cardiac remodeling and dysfunction. *Circulation*. 2020;141:217–233. doi:10.1161/CIRCULATIONAHA.119.042178
7. He X, Zeng H, Chen JX. Emerging role of SIRT3 in endothelial metabolism, angiogenesis, and cardiovascular disease. *J Cell Physiol*. 2019;234:2252–2265. doi:10.1002/jcp.27200
8. Hojo Y, Saito T, Kondo H. Role of apoptosis in left ventricular remodeling after acute myocardial infarction. *J Cardiol*. 2012;60:91–92. doi:10.1016/j.jjcc.2012.05.014
9. Sano M, Komuro I. p53と心不全発症 [P53 and its role in the development of heart failure]. *Japan J Clin Med*. 2008;66:1013–1021. Japanese.
10. Feng X, Liu X, Zhang W, Xiao W. p53 directly suppresses BNIP3 expression to protect against hypoxia-induced cell death. *EMBO J*. 2011;30:3397–3415. doi:10.1038/emboj.2011.248
11. Gogiraju R, Xu X, Bochenek ML, et al. Endothelial p53 deletion improves angiogenesis and prevents cardiac fibrosis and heart failure induced by pressure overload in mice. *J Americ Heart Assoc*. 2015;4. doi:10.1161/JAHA.115.001770
12. Katare PB, Nizami HL, Paramesha B, Dinda AK, Banerjee SK. Activation of toll like receptor 4 (TLR4) promotes cardiomyocyte apoptosis through SIRT2 dependent p53 deacetylation. *Sci Rep*. 2020;10:19232. doi:10.1038/s41598-020-75301-4
13. Zhang W, Zhang Y, Zhou D, Zhou S, Chen W. Clinical observation of "Ginseng-Gecko Powder" in treating congestive heart failure. *Shanghai J Traditional Chin Med*. 2010;44:59–61. doi:10.16305/j.1007-1334.2010.06.032
14. Yang J, Cao M, Yuan S. Treatment of chronic heart failure with Shenge Powder based on cardiopulmonary syndrome. *Tianjin J Traditional Chin Med*. 2019;36:27–30. doi:10.11656/j.issn.1672-1519.2019.01.08
15. Qiao S, Li G, Ding L, et al. Clinical observation on the adjunctive therapy with shenge powder treating 36 cases of chronic heart failure of heart and kidney yang deficiency syndrome. *J Traditional Chin Med*. 2020;61:1536–1540. doi:10.13288/j.11-2166/r.2020.17.015
16. Cui B, Zheng Y, Zhou X, et al. Repair of adult mammalian heart after damages by oral intake of Gu Ben Pei Yuan San. *Front Physiol*. 2019;10:607. doi:10.3389/fphys.2019.00607
17. Chang H, Li C, Wang Q, et al. QSKL protects against myocardial apoptosis on heart failure via PI3K/Akt-p53 signaling pathway. *Sci Rep*. 2017;7:16986. doi:10.1038/s41598-017-17163-x
18. Doering CW, Jalil JE, Janicki JS, et al. Collagen network remodelling and diastolic stiffness of the rat left ventricle with pressure overload hypertrophy. *Cardiovascul Res*. 1988;22:686–695. doi:10.1093/cvr/22.10.686
19. Liu Q, Qu HY, Zhou H, et al. Luhong formula has a cardioprotective effect on left ventricular remodeling in pressure-overloaded rats, evidence-based complementary and alternative medicine. *eCAM*. 2020;2020:4095967. doi:10.1155/2020/4095967
20. Xu S, Bian R, Chen X. *Experimental Methodology of Pharmacology*. Beijing: People's Health Publishing House; 2002.
21. Qiu B, Wei Y, Yuan S, et al. Protective effect of shen'ge powder on heart failure induced by pressure overload in rats and underlying mechanism. *Chin Archiv Tradit Chin Med*. 2022;40:54–57. doi:10.13193/j.issn.1673-7717.2022.04.010
22. Watanabe K, Ohta Y, Inoue M, et al. Bisoprolol improves survival in rats with heart failure. *J Cardiovascul Pharmacol*. 2001;38(1):S55–8. doi:10.1097/00005344-200110001-00012
23. Ni Y, Wang T, Zhuo X, et al. Bisoprolol reversed small conductance calcium-activated potassium channel (SK) remodeling in a volume-overload rat model. *Mol Cell Biochem*. 2013;384:95–103. doi:10.1007/s11010-013-1785-5
24. Huang C, Zhou S, Chen C, et al. Biodegradable redox-responsive aiegen-based-covalent organic framework nanocarriers for long-term treatment of myocardial ischemia/reperfusion injury. *Small*. 2022;18:e2205062. doi:10.1002/smll.202205062
25. Meng Q, Guo Y, Zhang D, Zhang Q, Li Y, Bian H. Tongsaimai reverses the hypertension and left ventricular remolding caused by abdominal aortic constriction in rats. *J Ethnopharmacol*. 2020;246:112154. doi:10.1016/j.jep.2019.112154
26. Mei Z, Wang X, Liu W, et al. Mitochondrial adaptations during myocardial hypertrophy induced by abdominal aortic constriction. *Cardiovas Pathol*. 2014;23:283–288. doi:10.1016/j.carpath.2014.05.003
27. Li YL, Ju JQ, Yang CH, Jiang HQ, Xu JW, Zhang SJ. Oral Chinese herbal medicine for improvement of quality of life in patients with chronic heart failure: a systematic review and meta-analysis. *Quality Life Res*. 2014;23:1177–1192. doi:10.1007/s11136-013-0582-7
28. Hao P, Jiang F, Cheng J, Ma L, Zhang Y, Zhao Y. Traditional Chinese medicine for cardiovascular disease: evidence and potential mechanisms. *J Amer Coll Cardiol*. 2017;69:2952–2966. doi:10.1016/j.jacc.2017.04.041
29. Kaufman DW, Kelly JP, Rosenberg L, Anderson TE, Mitchell AA. Recent patterns of medication use in the ambulatory adult population of the United States: the Slone survey. *JAMA*. 2002;287:337–344. doi:10.1001/jama.287.3.337
30. Pharand C, Ackman ML, Jackevicius CA, et al. Canadian cardiovascular pharmacists, use of OTC and herbal products in patients with cardiovascular disease. *Ann Pharmacoth*. 2003;37:899–904. doi:10.1345/aph.1C163
31. Nilsson M, Trehn G, Asplund K. Use of complementary and alternative medicine remedies in Sweden. A population-based longitudinal study within the northern Sweden MONICA Project. Multinational monitoring of trends and determinants of cardiovascular disease. *J Internal Med*. 2001;250:225–233. doi:10.1046/j.1365-2796.2001.00882.x
32. Zheng X, Wang S, Zou X, et al. Ginsenoside Rb1 improves cardiac function and remodeling in heart failure. *Experim Anim*. 2017;66:217–228. doi:10.1538/expanim.16-0121
33. Yang T, Miao Y, Zhang T, et al. Ginsenoside Rb1 inhibits autophagy through regulation of Rho/ROCK and PI3K/mTOR pathways in a pressure-overload heart failure rat model. *J Pharm Pharmacol*. 2018;70:830–838. doi:10.1111/jphp.12900
34. Wang T, Yu X, Qu S, Xu H, Han B, Sui D. Effect of ginsenoside Rb3 on myocardial injury and heart function impairment induced by isoproterenol in rats. *Eur J Pharmacol*. 2010;636:121–125. doi:10.1016/j.ejphar.2010.03.035
35. Eichhorn EJ, Domanski MJ, Krause-Steinrauf H, Bristow MR, Lavori PW. A trial of the beta-blocker bucindolol in patients with advanced chronic heart failure. *New Engl J Med*. 2001;344:1659–1667. doi:10.1056/NEJM200105313442202
36. Lechat PF, Brunhuber KW, Hofmann R, et al. The Cardiac Insufficiency Bisoprolol Study II (CIBIS-II): a randomised trial. *Lancet*. 1999;353:9–13. doi:10.1016/S0140-6736(98)11181-9
37. Reiken S, Wehrens XH, Vest JA, et al. Beta-blockers restore calcium release channel function and improve cardiac muscle performance in human heart failure. *Circulation*. 2003;107:2459–2466. doi:10.1161/01.CIR.0000068316.53218.49

38. Sari N, Katanasaka Y, Honda H, et al. Cacao bean polyphenols inhibit cardiac hypertrophy and systolic dysfunction in pressure overload-induced heart failure model mice. *Planta med*. 2020;86:1304–1312. doi:10.1055/a-1191-7970
39. De Boer RA, Pinto YM, Van Veldhuisen DJ. The imbalance between oxygen demand and supply as a potential mechanism in the pathophysiology of heart failure: the role of microvascular growth and abnormalities. *Microcirculation*. 2003;10:113–126. doi:10.1038/sj.mn.7800188
40. Marti CN, Gheorghiade M, Kalogeropoulos AP, Georgiopoulou VV, Quyyumi AA, Butler J. Endothelial dysfunction, arterial stiffness, and heart failure. *J Amer Coll Cardiol*. 2012;60:1455–1469. doi:10.1016/j.jacc.2011.11.082
41. Oka T, Akazawa H, Naito AT, Komuro I. Angiogenesis and cardiac hypertrophy: maintenance of cardiac function and causative roles in heart failure. *Circul Res*. 2014;114:565–571. doi:10.1161/CIRCRESAHA.114.300507
42. Semenza GL. Hypoxia-inducible factor 1 and cardiovascular disease. *Ann Rev Physiol*. 2014;76:39–56. doi:10.1146/annurev-physiol-021113-170322
43. Melincovici CS, Bosca AB, Susman S, et al. Vascular endothelial growth factor (VEGF) - key factor in normal and pathological angiogenesis. *Roman J Morphol Embryol*. 2018;59:455–467.
44. Fitzpatrick JR, Frederick JR, McCormick RC, et al. Tissue-engineered pro-angiogenic fibroblast scaffold improves myocardial perfusion and function and limits ventricular remodeling after infarction. *J Thoracic Cardiovasc Surg*. 2010;140:667–676. doi:10.1016/j.jtcvs.2009.12.037
45. Chang JH, Jin MM, Liu JT. Dexmedetomidine pretreatment protects the heart against apoptosis in ischemia/reperfusion injury in diabetic rats by activating PI3K/Akt signaling in vivo and in vitro. *Biomed Pharmac*. 2020;127:110188. doi:10.1016/j.biopha.2020.110188
46. Sun Y, Su Q, Li L, Wang X, Lu Y, Liang J. MiR-486 regulates cardiomyocyte apoptosis by p53-mediated BCL-2 associated mitochondrial apoptotic pathway. *BMC Cardiovascul Disord*. 2017;17:119. doi:10.1186/s12872-017-0549-7
47. Zheng N, Li H, Wang X, Zhao Z, Shan D. Oxidative stress-induced cardiomyocyte apoptosis is associated with dysregulated Akt/p53 signaling pathway. *J Recept Sign Transd Res*. 2020;40:599–604. doi:10.1080/10799893.2020.1772297
48. van Empel VP, Bertrand AT, Hofstra L, Crijns HJ, Doevendans PA, De Windt LJ. Myocyte apoptosis in heart failure. *Cardiovascul Res*. 2005;67:21–29. doi:10.1016/j.cardiores.2005.04.012
49. Pepe M, Mamdani M, Zentilin L, et al. Intramyocardial VEGF-B167 gene delivery delays the progression towards congestive failure in dogs with pacing-induced dilated cardiomyopathy. *Circul Res*. 2010;106:1893–1903. doi:10.1161/CIRCRESAHA.110.220855
50. Zhou CH, Zhang XP, Liu F, Wang W. Modeling the interplay between the HIF-1 and p53 pathways in hypoxia. *Sci Rep*. 2015;5:13834. doi:10.1038/srep13834
51. Wang P, Guan D, Zhang XP, Liu F, Wang W. Modeling the regulation of p53 activation by HIF-1 upon hypoxia. *FEBS Lett*. 2019;593:2596–2611. doi:10.1002/1873-3468.13525